A Designed Photoenzyme Promotes Enantioselective [2+2]-Cycloadditions *via* Triplet Energy Transfer

Jonathan S. Trimble,[1†] Rebecca Crawshaw,[1†] Florence J. Hardy,[1] Colin W. Levy,[1] Murray J.B. Brown,[2] Douglas E. Fuerst,[3] Derren J. Heyes,[1] Richard Obexer,[1] Anthony P. Green[1*]

[*] - Corresponding author
[†] - these authors contributed equally
[1]Department of Chemistry & Manchester Institute of Biotechnology, The University of Manchester, 131 Princess Street, Manchester, M1 7DN, U.K.
[2]Synthetic Biochemistry, Medicinal Science and Technology, GlaxoSmithKline Medicines Research Centre, Stevenage, U.K.
[3]Synthetic Biochemistry, Medicinal Science & Technology, GlaxoSmithKline, Collegeville, PA, U.S.A.

Abstract

The ability to programme new modes of catalysis into proteins would allow the development of enzyme families with functions beyond those found in nature. To this end, genetic code expansion methodology holds particular promise, as it allows the site-selective introduction of new functional elements into proteins as non-canonical amino acid side chains. Here, we exploit an expanded genetic code to develop a photoenzyme that operates *via* triplet energy transfer catalysis, a versatile mode of reactivity in organic synthesis that is currently not accessible to biocatalysis. Installation of a genetically encoded photosensitiser into the beta-propeller scaffold of DA_20_00 converts a *de novo* Diels-Alderase into a photoenzyme for [2+2]-cycloadditions (EnT1.0). Subsequent development and implementation of a platform for photoenzyme evolution afforded an efficient and enantioselective enzyme (EnT1.3, up to 99% *e.e.*) that can promote selective cycloadditions that have proven challenging to achieve with small molecule catalysts. EnT1.3 performs >300 turnovers and, in contrast to small molecule photocatalysts, can operate effectively under aerobic conditions. A 1.7 Å resolution X-ray crystal structure of an EnT1.3-product complex shows how multiple functional components work in synergy to promote efficient and selective photocatalysis. This study opens the door to a wealth of new excited-state chemistry in protein active sites and establishes the framework for developing a new generation of evolvable photocatalysts with efficiencies and specificities akin to natural enzymes.

Introduction

Triplet energy transfer (EnT) photocatalysis promotes a broad range of valuable chemical transformations including cycloadditions, electrocyclic reactions, deracemizations, migrations, and rearrangements, many of which are not accessible from the ground state.[1–8] Photons offer a convenient and tuneable source of energy to selectively access reactive excited state intermediates under mild reaction conditions. Perhaps the most prominent class of photochemical reactions are [2+2]-cycloadditions, which construct cyclobutanes, oxetanes and azetidines.[9–11] In contrast to the analogous Diels-Alder [4+2]-cycloadditions, [2+2]-cycloadditions are thermally forbidden due to incompatible ground state orbital symmetries (Figure 1A). The key stages of EnT photocatalysis are shown in Figure 1B. Light energy is used to promote a triplet sensitiser from the ground state (S_0) to a singlet excited state (S_1), which then undergoes intersystem crossing to a triplet state (T_1). Since relaxation from T_1 to S_0 is spin-forbidden, triplet intermediates are relatively long-lived compared with singlet excited states. Commonly employed triplet photosensitisers include conjugated aromatic ketones such as benzophenone, xanthone, and thioxanthone, which display high quantum efficiencies for population of

the triplet state. The next step involves energy transfer from the triplet photosensitiser to the substrate in an overall spin-allowed process that returns the photosensitiser to the S_0 level and simultaneously promotes the substrate from S_0 to the reactive T_1 state, which can then undergo a variety of intra- and intermolecular processes.[2,3]

Enantioselective versions of photochemical reactions have been developed through dual catalytic strategies that combine an achiral photosensitiser with a photochemically inactive chiral catalyst (Figure 1C),[12–14] or by employing chiral photosensitisers (Figure 1D).[10,15] Although powerful, these approaches do not offer a general solution, and many desirable photochemical processes are not amenable to enantioselective catalysis. Furthermore, these reactions are oxygen sensitive, often require high catalyst loadings, and are restricted to a narrow range of substrates, with even small structural changes leading to substantial reductions in activity or selectivity.[16] In principle, enzyme active sites could offer more versatile chiral environments for mediating enantioselective photochemistry, where multiple functional elements can be accurately positioned within a single pocket. Through directed evolution these active sites could be sculpted to maximise productive interactions between the protein, substrate and photosensitiser, to deliver efficient and selective photocatalysts (Figure 1E). However, while a handful of natural photoenzymes[17–20] and engineered biocatalysts[21–26] are known to operate *via* photo-induced electron transfer, enzymes that operate through EnT are currently unknown.

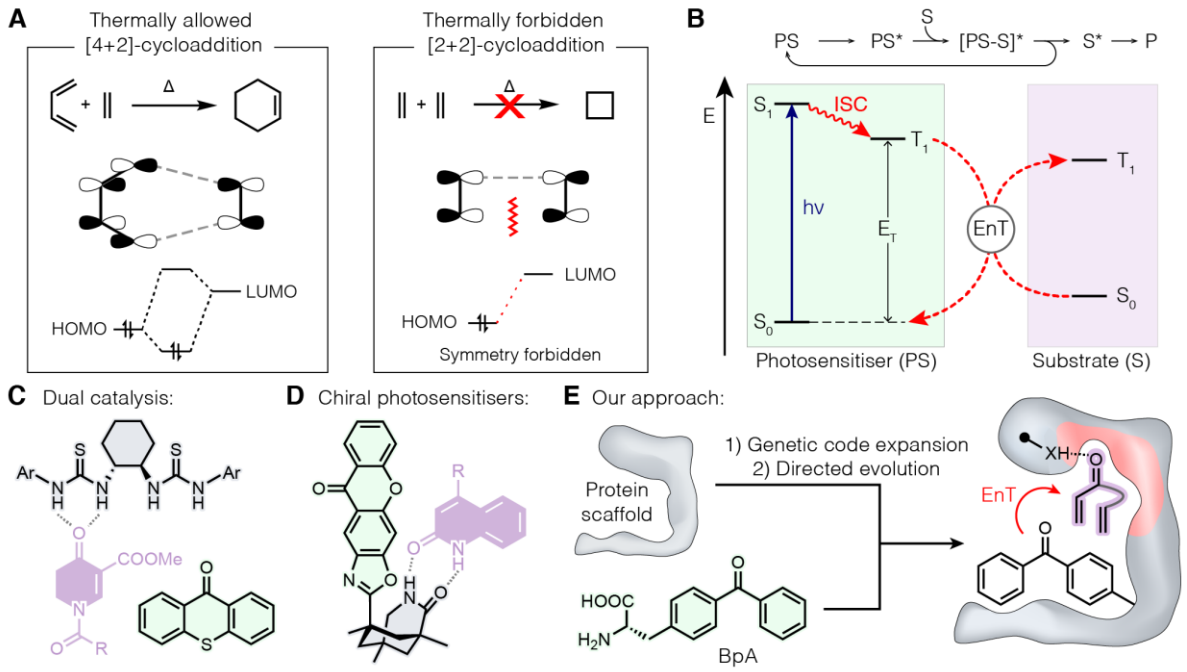

Figure 1. Photochemistry of [2+2]-cycloadditions. A. Comparison of thermally allowed [4+2]- and thermally forbidden [2+2]-cycloadditions and their ground state orbital interactions. **B.** Jablonski diagram representation of EnT photocatalysis. A photosensitiser (PS) is excited into a singlet state (S_1), which subsequently undergoes intersystem crossing (ISC) to the triplet state (T_1). EnT returns the PS to ground state, while exciting the substrate into T_1. **C-D.** Enantioselective EnT photocatalysis can be achieved using achiral photosensitisers in combination with chiral co-catalysts[13,14] or using chiral photosensitisers.[15] **E.** The approach to photoenzyme development described in this manuscript, involving selective installation of a genetically encoded photosensitiser into a protein scaffold and subsequent optimisation of the modified protein by directed evolution.

Results and Discussion

To develop a selective photoenzyme, we chose the computationally designed Diels-Alderase DA_20_00 as a host scaffold due to mechanistic similarities between [4+2]- and [2+2]-cycloadditions.[27] The DA_20_00 active site contains designed hydrogen bonding residues (Tyr121 and Gln195) intended to promote the Diels-Alder reaction, which may prove useful in supporting catalysis of [2+2]-cycloadditions. These residues are embedded within a large hydrophobic pocket suitable for accommodating a bulky aromatic photosensitiser (Figure 2A). To unlock photocatalytic activity, an engineered *Methanococcus jannaschii* tyrosyl-tRNAsynthetase/tyrosyl-tRNA (*Mj*TyrRS/*Mj*tRNA^{Tyr}) pair was used to incorporate 4-benzoylphenylalanine (BpA) at several positions around the DA_20_00 active site pocket (Extended Data Figure 1).[28] Intramolecular [2+2]-cycloaddition of quinolone **1** was selected as the target transformation (Figure 2B).[15] Benzophenone (BP) is a suitable photosensitiser for this reaction and gives rise to racemic straight and crossed chain products (**1a** and **1b**) as a 1.4:1 mixture of regioisomers (Figure 2C). Placement of BpA at position 173 within the hydrophobic pocket of DA_20_00 provided the active photoenzyme EnT1.0, which is a more effective catalyst than BP and displays modest levels of regio- (2:1, **1a**:**1b**) and enantioselectivity (46% *e.e.* for the major product (-)-**1a**). EnT1.0 activity is strictly dependent on light and the presence of the BpA173 photosensitiser (Figure 2C).

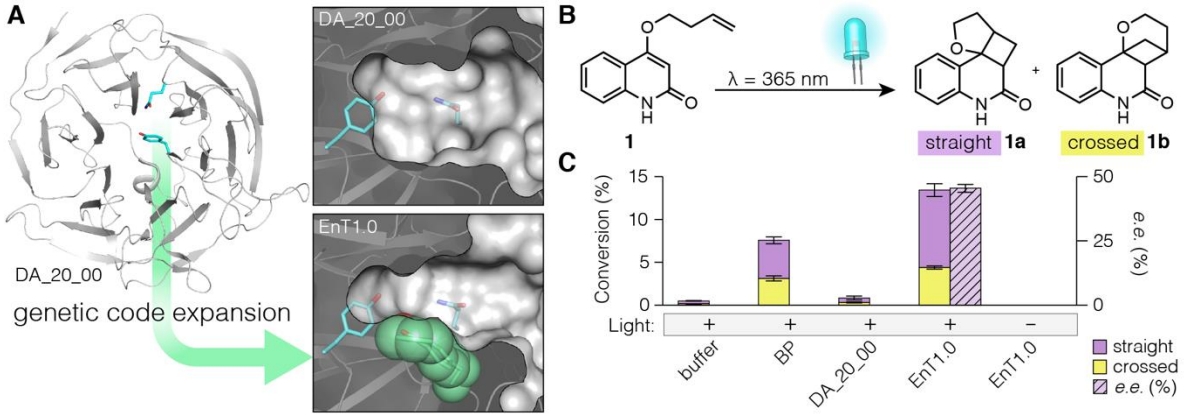

Figure 2. Development of the first-generation photoenzyme, EnT1.0. A. Genetic incorporation of a BpA photosensitiser (green CPK spheres) into the hydrophobic core of DA_20_00 (PDB: 3I1C) afforded the first-generation photocatalyst EnT1.0 (PDB: 7ZP5). **B.** Intramolecular [2+2]-photocycloaddition of 4-(but-3-en-1-yloxy)quinolin-2(1H)-one (**1**) gives rise to two regioisomeric products, 3,3a,4,4a-tetrahydro-2H-furo[2',3':2,3]cyclobuta[1,2-c]quinolin-5(6H)-one (**1a**) and 2,3,4,4a-tetrahydro-4,10b-methanopyrano[3,2-c]quinolin-5(6H)-one (**1b**) **C.** Bar chart showing the conversion of **1** to **1a** and **1b** by EnT1.0, BP, and the unmodified protein DA_20_00. Reaction conditions: 15 µM catalyst, 400 µM **1**, 30 minutes irradiation at 365 nm, 4 °C. EnT1.0 activity is dependent on light and affords the major product (-)-**1a** with 46% *e.e.*. Conversion and selectivity data are given in SI Table S1. Error bars represent the standard deviation of measurements made in triplicate.

To improve EnT1.0 activity, we initially mutated eight residues that lie in proximity to BpA173 to alanine (Extended Data Figure 2). An M90A mutation gave rise to a substantial 3-fold increase in conversion to **1a** along with a modest improvement in enantioselectivity to 60% *e.e.* (EnT1.1, Figure 3, Extended Data Figure 2). This improved variant facilitated detection of enzyme activity in clarified cell

lysate, and enabled the development of a directed evolution workflow suitable for high-throughput engineering of triplet energy transfer photoenzymes. This evolutionary workflow relies on uniform irradiation of enzyme variants arrayed in microtiter plates, which was achieved using a commercial LED array (see Experimental Procedures). The observed coefficient of variance across an assay plate using purified EnT1.0 was shown to be less than 5% (Supplementary Figure S1), a value that is in line with established high-throughput screening methods.

The evolutionary strategy consisted of two rounds of saturation mutagenesis targeting residues in the active site and second coordination sphere, which were individually randomised using NNK degenerate codons. Individual variants arrayed in 96-well microtiter plates were irradiated for 30 mins at 365nm using an LED array in the presence of substrate **1** and reactions analysed by high-throughput ultra-performance liquid chromatography (UPLC, SI Figure S2-3). The most active (~1%) clones, identified based on conversion to **1a**, were then evaluated as purified proteins for improved activity and enantioselectivity (SI Figure 4). Beneficial mutations identified during each round were subsequently combined by DNA shuffling. Following evaluation of ~3500 library members, an EnT1.3 variant emerged with improved activity, stability, and selectivity. EnT1.3 contains five mutations (EnT1.0 M90A Q149D P196R K225E A229S, Extended Data Figure 3) and achieves a substantial 10-fold improvement in reaction conversion of **1** to **1a** compared with EnT1.0 following 30 minutes of irradiation (Figure 3C & 3D). The enhanced performance of EnT1.3 arises from a combination of a 4-fold increase in initial rate (Extended Data Figure 4), improved regioselectivity (**1a**:**1b** 2:1 for EnT1.0 vs 9:1 for EnT1.3, Figure 3C), and reduced susceptibility to photo-deactivation, that likely arises in EnT1.0 from an intramolecular photo-crosslinking process involving the benzophenone side chain (Extended Data Figure 5). EnT1.3 also offers high levels of enantio-control, generating (-)-**1a** with >99% *e.e.*. Interestingly, EnT1.3 is more active at 4 °C than at room temperature (Extended Data Figure 6), which may reflect an increased lifetime of the photosensitiser triplet state at lower temperatures.[29] In contrast to small-molecule photocatalysts, which are highly sensitive to oxygen due to triplet quenching, EnT1.3 is tolerant of aerobic buffers (Figure 3D) and can achieve >300 turnovers under these conditions (Extended Data Figure 7). With only 1.5 mol% EnT1.3, near complete conversion of **1** to optically pure (-)-**1a** can be achieved within 2 hr (SI Table S3), underscoring the efficiency of our engineered photoenzyme.

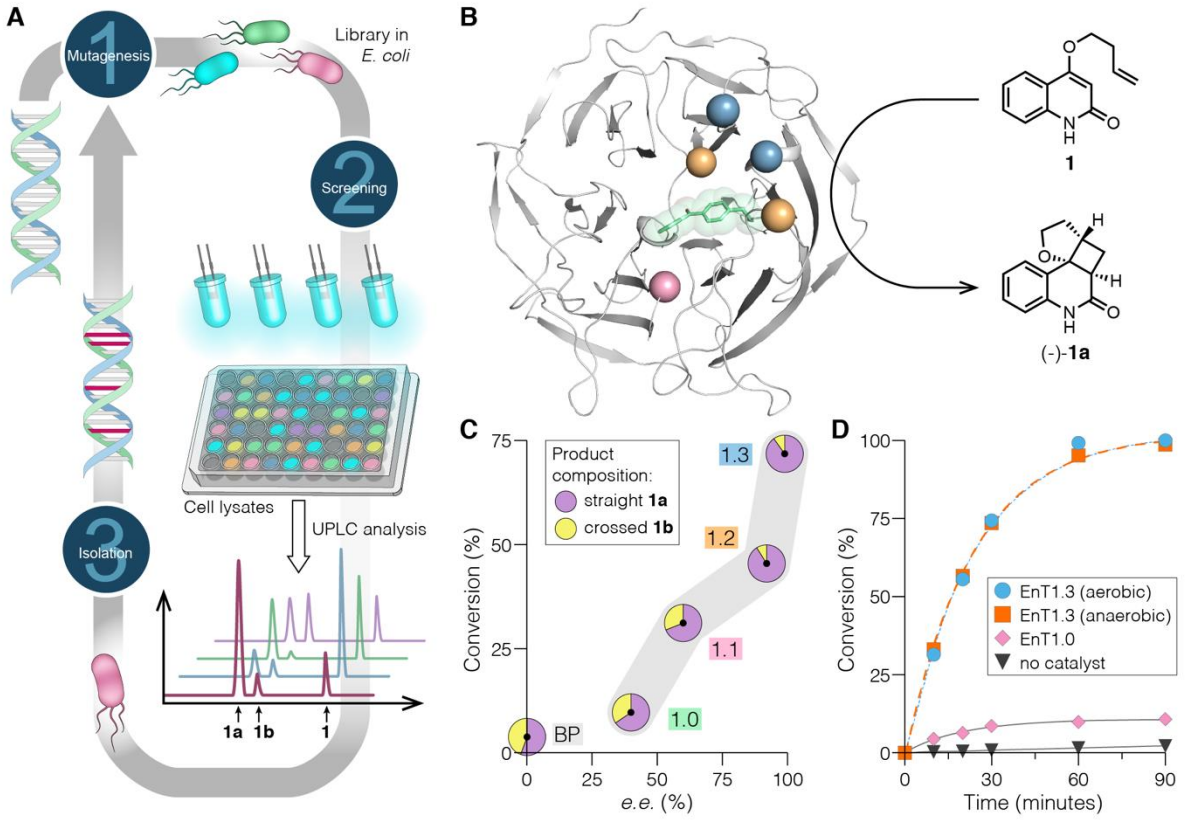

Figure 3: Directed evolution of an efficient and enantioselective photoenzyme. A. Schematic of the directed evolution workflow for photoenzyme engineering. **B.** Mutational map of EnT1.3, highlighting the encoded photosensitiser BpA173 (green sticks and semi-transparent CPK spheres) and residues installed during alanine scanning (pink sphere) and rounds 1 and 2 of evolution (peach and blue spheres, respectively). **C.** Reaction conversion, regioselectivity, and enantioselectivity were improved along the evolutionary trajectory. Reaction conditions: 10 μM catalyst (2.5 mol%), 400 μM **1**, 30 minutes irradiation at 365 nm, 4 °C. The ratio of **1a**:**1b** is represented as a pie chart and *e.e.* is given for (-)-**1a**. All conversion and selectivity data, including standard deviations, are given in Extended Data Figure 8. **D.** Reaction time-courses (**1** to **1a** and **1b,** 10 μM catalyst (2.5 mol%), 400 μM **1**, 365 nm, 4 °C) catalysed by Ent1.0 (pink) and EnT1.3 (blue). A comparison of EnT1.3 activity under anaerobic conditions is shown in orange.

We next explored the photocatalytic activity of EnT1.3 towards [2+2]-cycloadditions of allyloxy-, alken-1-yl-, and allyloxy(methyl)- quinolones to generate optically enriched products (**2a**-**12a**, Figure 4). High conversions and selectivities were achieved in the majority of cases. With substrates **3**, **7** and **11**, introduction of a gem-dimethyl moiety led to a reduction in enantioselectivity and in these cases EnT1.2 proved to be a more selective photocatalyst. The ability of EnT1.3 to generate **2a** and **6a** with high levels of stereocontrol is particularly noteworthy. Analogous reactions with small chiral photosensitisers proceed with poor selectivity, as cyclizations to form 6-membered ring analogues are relatively slow and competing dissociation of the excited substrate from the photosensitiser erodes *e.e.*.[2,10,16] Small molecule chiral photosensitisers also rely on complementary dual hydrogen-bonding contacts between the substrate and catalyst to achieve enantioselective photochemistry.[15] To demonstrate that protein catalysts are not constrained in the same manner, we next investigated cycloaddition of an *N*-methyl derivative **12**. EnT1.3 affords optically enriched **12a**, along with its

regioisomer **12b**, with modest selectivity (2:1 r.r., 36% *e.e.* for **12a**), which could be further enhanced (4:1 r.r., 78% *e.e.* for **12a**) by introducing a rational Y121F mutation (*vide infra*). This example demonstrates how protein active sites can be readily adapted to augment catalytic function and suggests that our photoenzymes can mediate selective transformations of substrate classes that are beyond the reach of existing small-molecule systems.

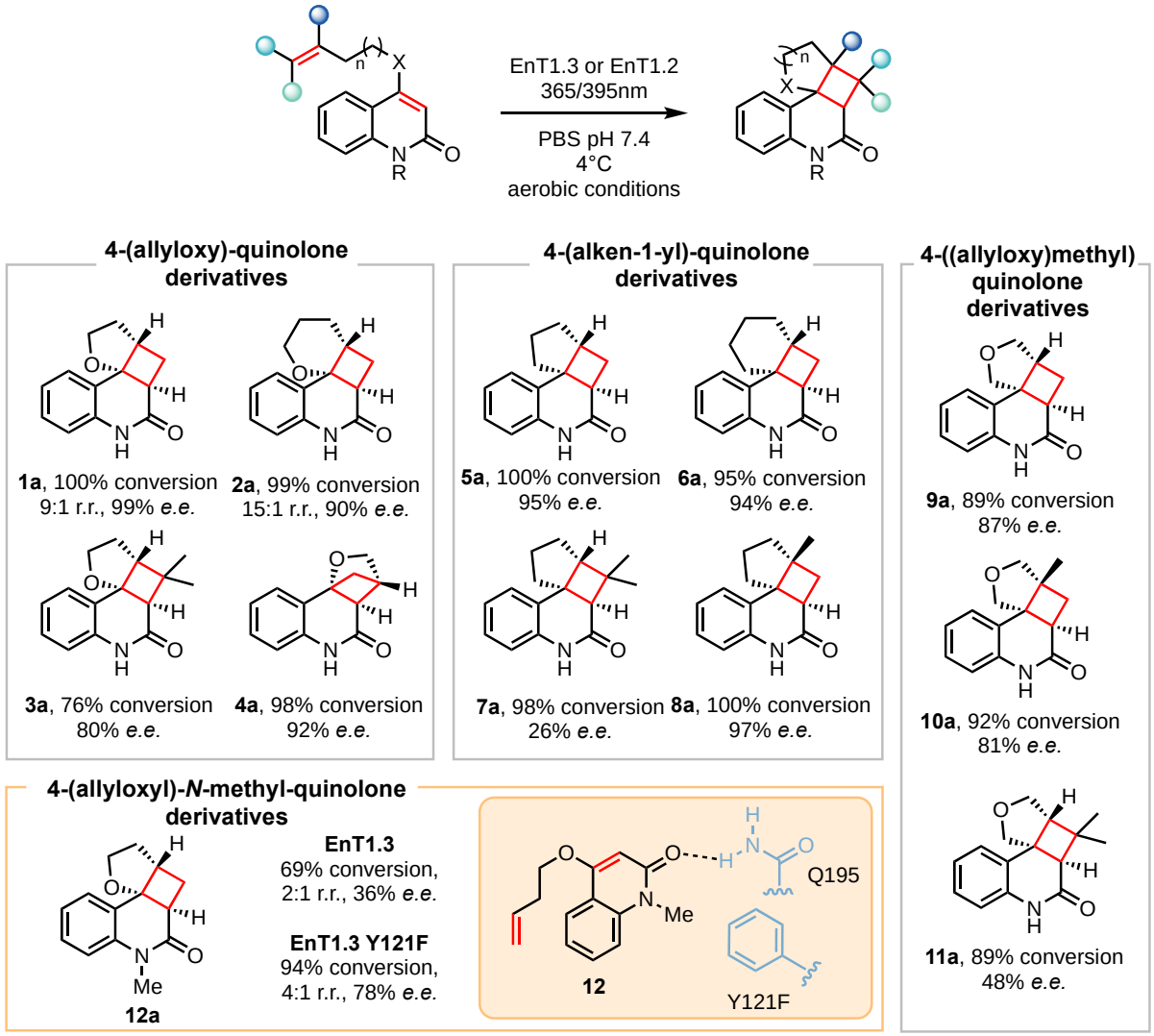

Figure 4: Substrate scope of EnT1.3 and selected variants. EnT1.3 promotes intramolecular [2+2]-cycloadditions on a range of quinolones to produce 4-(allyloxy)-, 4-(alken-1-yl)- and 4-((allyloxy)methyl)-quinolone derivatives **1a-2a**, **4a-6a**, and **8a-10a** with high conversions and excellent selectivities. Reactions to produce **3a**, **7a** and **11a** are performed with EnT1.2, which gave higher levels of selectivity compared with EnT1.3. With *N*-methyl quinolone **12**, reactions with EnT1.3 proceed with modest selectivity, which can be improved with a rational Y121F mutation. Reaction conversions are the mean of biotransformations performed in triplicate. The absolute stereochemistry of products **2a-12a** were assigned by analogy to the product (-)-**1a** formed by EnT1.3. Reaction conditions for the synthesis of **1a**–**12a** are presented in SI Table S3.

To gain insights into the EnT1.3 catalytic mechanism, a crystal structure of a C-terminally truncated analogue (EnT1.3ΔC$_{310-314}$, see Supporting Information) complexed with product (-)-**1a** was solved (1.7 Å, Figure 5, Supplementary Table S5). This truncation has negligible effect on catalytic activity or selectivity (Supplementary Figure S5), and was introduced to circumvent the C-terminus of a neighbouring chain from occluding the EnT1.3 active site *in crystallo*. The ligand sits in a snug active site pocket with its aromatic ring sandwiched between His287 and the benzophenone sidechain (3.6 Å and 3.8 Å respectively, Figure 5, Supplementary Information Figure S6). This pose presumably allows for efficient triplet energy transfer from the excited-state photosensitiser to the parent substrate. The crystal structure suggests that Trp244 may play a role in controlling reaction selectivity in favour of the formation of (-)-**1a** by shaping the active site cavity to prevent addition of the exocyclic alkene to the enantiotopic face of the excited quinolone. Indeed, a W244A mutation leads to a substantial reduction in activity and racemic product formation (Extended Data Figure 8). Ligand binding is further supported by complementary hydrogen bonding interactions with Tyr121, which serves as a hydrogen bond acceptor to the quinolone N-H, and Gln195, which acts as a hydrogen bond donor to the quinolone carbonyl (Figure 5). Interestingly, Tyr121 and Gln195 were designed to mediate Diels-Alder catalysis in DA_20_00 through hydrogen bonding interactions, albeit with opposite donor/acceptor relationships to those observed in EnT1.3. With substrate **1**, mutation of Tyr121 to Phe leads to a 3-fold reduction in activity along with a modest decrease in enantioselectivity (67% *e.e.*, Extended Data Figure 8). In contrast, this mutation improves both activity and selectivity towards *N*-methylated substrate **12** (Figure 4), where the *N*-methyl substituent likely occupies the position vacated by removal of the Tyr121 phenolic oxygen. The hydrogen bond from Gln195 to the quinolone carbonyl is particularly short (2.6 Å) and likely serves to lower the triplet energy of the substrate.[30] Mutation of Gln195 to Ala leads to a considerable reduction in activity and selectivity, underscoring its importance to EnT1.3 catalysis. Gln195 is anchored in position by an additional hydrogen bond with Arg196, which emerged during evolution. Interestingly, in apo-EnT1.3 Gln195 and Arg196 lie in markedly different orientations, with Arg196 instead interacting with Asp149 and Glu225, suggesting that substrate binding may induce formation of a productive Arg196-Gln195-substrate hydrogen bonding network (Extended Data Figure 9). This combined structural analysis offers a first glimpse into active site features governing efficient energy transfer catalysis, and provides an important blueprint for the future design of photoenzymes with new and augmented functions.

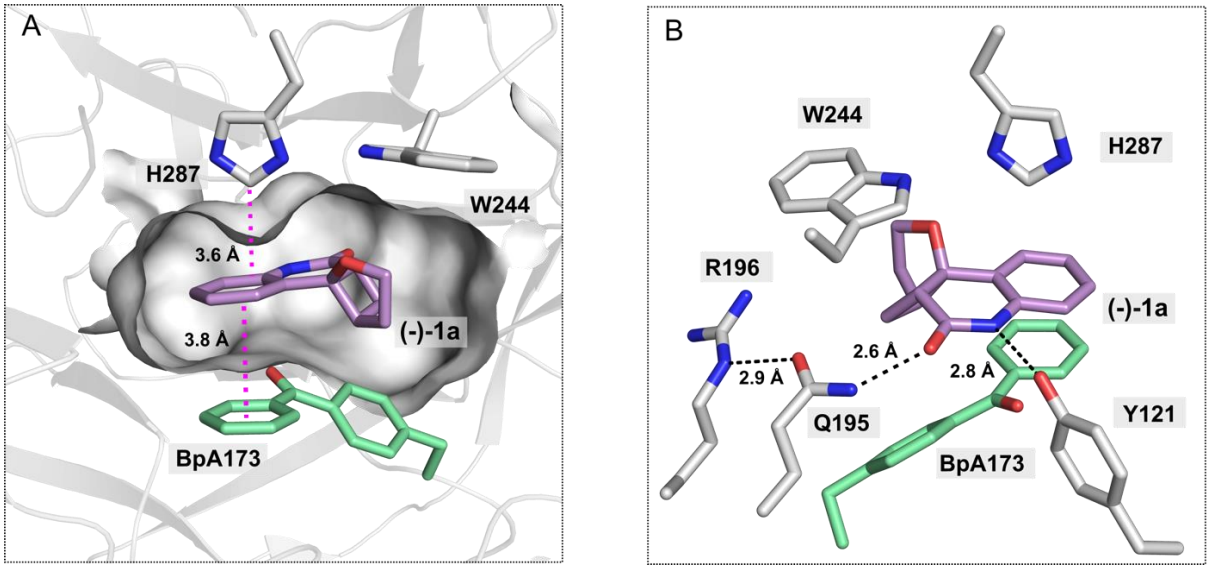

Figure 5: A 1.7 Å crystal structure of EnT1.3ΔC$_{310-314}$ in complex with product (-)-1a. A. The product (atom-coloured sticks, carbon purple) is well accommodated within the active site pocket

(shown as a grey surface) in proximity to the BpA173 sidechain (atom-coloured sticks with green carbon), His287 and Trp244 (atom-coloured sticks, with grey carbon). π–stacking interactions are shown as pink dashed lines. **B.** Expanded view of the active site showing hydrogen bonding interactions (black dashed lines) involving R196, Q195, Y121 and the ligand.

In summary, our study provides a powerful demonstration of how an expanded genetic code can be used to embed entirely new modes of catalysis into proteins. This technology has allowed the development of a proficient photoenzyme that operates via a triplet energy transfer mechanism, a versatile reaction manifold in organic synthesis that was previously inaccessible to biocatalysis. While EnT1.3 was tailored to promote photochemical [2+2]-cycloadditions, we anticipate that our approach can be readily adapted to alternative chemistries that are enabled by triplet energy transfer. The catalytic performance and structural sophistication of EnT1.3 is particularly notable, given that <1000 protein variants were evaluated across the evolutionary trajectory. Presumably, more efficient photocatalysts will be generated through a deeper exploration of protein sequence. Likewise, combinations of high-throughput experimentation and *in silico* design will deliver active sites with new geometries and arrangements of functional groups suitable for mediating selective photocatalysis.[31] Thus with the mechanistic framework for embedding EnT catalysis into proteins now established, we are optimistic about the prospect of developing photoenzymes for a broad array of valuable photochemical processes.

References

1. Tröster, A., Bauer, A., Jandl, C. & Bach, T. Enantioselective Visible-Light-Mediated Formation of 3-Cyclopropylquinolones by Triplet-Sensitized Deracemization. *Angew. Chem. Int. Ed.* **58**, 3538–3541 (2019).

2. Großkopf, J., Kratz, T., Rigotti, T. & Bach, T. Enantioselective Photochemical Reactions Enabled by Triplet Energy Transfer. *Chem. Rev.* **122**, 1626–1653 (2022).

3. Strieth-Kalthoff, F. & Glorius, F. Triplet Energy Transfer Photocatalysis: Unlocking the Next Level. *Chem* **6**, 1888–1903 (2020).

4. Kleinmans, R. *et al.* Intermolecular [2π+2σ]-photocycloaddition enabled by triplet energy transfer. *Nature* (2022). doi:10.1038/s41586-022-04636-x

5. Alonso, R. & Bach, T. A Chiral Thioxanthone as an Organocatalyst for Enantioselective [2+2] Photocycloaddition Reactions Induced by Visible Light. *Angew. Chem. Int. Ed.* **53**, 4368–4371 (2014).

6. Münster, N., Parker, N. A., van Dijk, L., Paton, R. S. & Smith, M. D. Visible Light Photocatalysis of 6π Heterocyclization. *Angew. Chem. Int. Ed. Engl.* **56**, 9468–9472 (2017).

7. Huang, M., Zhang, L., Pan, T. & Luo, S. Deracemization through photochemical *E*/*Z* isomerization of enamines. *Science* **375**, 869–874 (2022).

8. Maturi, M. M., Pöthig, A. & Bach, T. Enantioselective Photochemical Rearrangements of Spirooxindole Epoxides Catalyzed by a Chiral Bifunctional Xanthone. *Aust. J. Chem.* **68**, 1682–1692 (2015).

9. Becker, M. R., Richardson, A. D. & Schindler, C. S. Functionalized azetidines via visible light-enabled aza Paternò-Büchi reactions. *Nat. Commun.* **10**, 5095 (2019).

10. Müller, C. *et al.* Enantioselective Intramolecular [2 + 2]-Photocycloaddition Reactions of 4-Substituted Quinolones Catalyzed by a Chiral Sensitizer with a Hydrogen-Bonding Motif. *J. Am. Chem. Soc.* **133**, 16689–16697 (2011).

11. Vogt, F., Jödicke, K., Schröder, J. & Bach, T. Paternò–Büchi Reactions of Silyl Enol Ethers and Enamides. *Synthesis* **24**, 4268–4273 (2009).

12. Blum, T. R., Miller, Z. D., Bates, D. M., Guzei, I. A. & Yoon, T. P. Enantioselective photochemistry through Lewis acid catalyzed triplet energy transfer. *Science* **354**, 1391–1395 (2016).

13. Mayr, F., Brimioulle, R. & Bach, T. A Chiral Thiourea as a Template for Enantioselective Intramolecular [2 + 2] Photocycloaddition Reactions. *J. Org. Chem.* **81**, 6965–6971 (2016).

14. Hörman, F. M. *et al.* Triplet Energy Transfer from Ruthenium Complexes to Chiral Eniminium Ions: Enantioselective Synthesis of Cyclobutanecarbaldehydes by [2+2] Photocycloaddition. *Angew. Chem. Int. Ed* **59**, 9659–9668 (2020).

15. Müller, C., Bauer, A. & Bach, T. Light-driven enantioselective organocatalysis. *Angew. Chem. Int. Ed. Engl.* **48**, 6640–6642 (2009).

16. Maturi, M. M. *et al.* Intramolecular [2+2] Photocycloaddition of 3- and 4-(But-3-enyl)oxyquinolones: Influence of the Alkene Substitution Pattern, Photophysical Studies, and Enantioselective Catalysis by a Chiral Sensitizer. *Chem. Eur. J.* **19**, 7461–7472 (2013).

17. Sorigué, D. *et al.* An algal photoenzyme converts fatty acids to hydrocarbons. *Science* **357**, 903–907 (2017).

18. Heyes, D. J. *et al.* Photochemical Mechanism of Light-Driven Fatty Acid Photodecarboxylase.

ACS Catal. **10**, 6691–6696 (2020).

19. Heyes, D. J. *et al.* Photocatalysis as the 'master switch' of photomorphogenesis in early plant development. *Nat. Plants* **7**, 268–276 (2021).

20. Tan, C. *et al.* The molecular origin of high DNA-repair efficiency by photolyase. *Nat. Commun.* **6**, 7302 (2015).

21. Liu, X. *et al.* A genetically encoded photosensitizer protein facilitates the rational design of a miniature photocatalytic CO_2-reducing enzyme. *Nat. Chem.* **10**, 1201–1206 (2018).

22. Black, M. J. *et al.* Asymmetric redox-neutral radical cyclization catalysed by flavin-dependent 'ene'-reductases. *Nat. Chem.* **12**, 71–75 (2020).

23. Gao, X., Turek-Herman, J. R., Choi, Y. J., Cohen, R. D. & Hyster, T. K. Photoenzymatic Synthesis of α-Tertiary Amines by Engineered Flavin-Dependent "Ene"-Reductases. *J. Am. Chem. Soc.* **143**, 19643–19647 (2021).

24. Emmanuel, M. A., Greenberg, N. R., Oblinsky, D. G. & Hyster, T. K. Accessing non-natural reactivity by irradiating nicotinamide-dependent enzymes with light. *Nature* **540**, 414–417 (2016).

25. Huang, X. *et al.* Photoinduced chemomimetic biocatalysis for enantioselective intermolecular radical conjugate addition. *Nat. Catal.* (2022). doi:10.1038/s41929-022-00777-4

26. Huang, X. *et al.* Photoenzymatic enantioselective intermolecular radical hydroalkylation. *Nature* **584**, 69–74 (2020).

27. Siegel, J. B. *et al.* Computational Design of an Enzyme Catalyst for a Stereoselective Bimolecular Diels-Alder Reaction. *Science* **329**, 309–313 (2010).

28. Chin, J. W., Martin, A. B., King, D. S., Wang, L. & Schultz, P. G. Addition of a photocrosslinking amino acid to the genetic code of Escherichia coli. *Proc. Natl. Acad. Sci. U. S. A.* **99**, 11020–11024 (2002).

29. Godfrey, T. S., Hilpern, J. W. & Porter, G. Triplet-triplet absorption spectra of benzophenone and its derivatives. *Chem. Phys. Lett.* **1**, 490–492 (1967).

30. Daub, M. E. *et al.* Enantioselective [2+2] Cycloadditions of Cinnamate Esters: Generalizing Lewis Acid Catalysis of Triplet Energy Transfer. *J. Am. Chem. Soc.* **141**, 9543–9547 (2019).

31. Lovelock, S. L. *et al.* The Road to Fully Programmable Protein Catalysts. *Nature* (2022). doi:10.1038/s41586-022-04456-z

Data Availability Statement

Coordinates and structure factors have been deposited in the Protein Data Bank under accession numbers 7ZP5, 7ZP6 and 7ZP7. The authors declare that the data supporting the findings of this study are available within the paper and its Supplementary Information files. Source data are available from the corresponding author upon reasonable request.

Acknowledgements

We acknowledge the European Research Council (ERC Starter Grant no. 757991 to A.P.G.) and the Biotechnology and Biological Sciences Research Council (David Phillips Fellowship BB/M027023/1 to A.P.G. and Transition Award BB/W014483/1). J.S.T was supported by an integrated catalysis Doctoral Training Programme (EP/023755/1). R.C was supported by a BBSRC Flexible Talent Mobility Account Award (BB/S507969/1). We are grateful to the Diamond Light Source for time on beamline i03 under proposal MX24447, to the Manchester SYNBIOCHEM Centre (BB/M017702/1), the Future Biomanufacturing Hub (EP/S01778X/1) and the Henry Royce Institute for Advanced

Materials (funded through EPSRC grants nos. EP/R00661X/1, EP/S019367/1, EP/P025021/1 and EP/P025498/1) for access to their facilities, and to M. Dunstan (Manchester Institute of Biotechnology) for guidance on automating directed evolution workflows. We thank R. Spiess and R. Sung (Manchester Institute of Biotechnology) for acquiring protein mass spectra and for assistance with UPLC method development, and Reach Separations (Nottingham) for supplying individual enantiomers of the product **1a**. We are grateful to GlaxoSmithKline for access to their facilities, and to Joseph Hosford and Lee J. Edwards (GlaxoSmithKline, Stevenage) for helpful discussions. We are also grateful to Prof. Daniele Leonori for helpful discussions throughout the project.

Author Contributions

J.S.T carried out organic synthesis and substrate profiling of EnT variants. R.C. carried out molecular biology, directed evolution experiments and protein crystallisation. J.S.T and R.C carried out protein production, assay development and photochemical assays. F.J.H. and C.L. interpreted, analysed and presented structural data. R.O., D.H., M.J.B.B., and D.F. contributed to experimental design and data analysis. A.P.G, J.S.T, R.C. F.J.H, and R.O. discussed the results and participated in writing the manuscript. All authors provided input throughout project progression. A.P.G. initiated and directed the research.

Competing Interests

The authors declare no competing interests.

Additional Information

Supplementary Information is available for this paper. Correspondence and requests for materials should be addressed to anthony.green@manchester.ac.uk.